ELSEVIER

Applied Surface Science 197–198 (2002) 639–643

applied surface science

www.elsevier.com/locate/apsusc

Engineering of a magnetic anisotropy using particles embedded in nano-multilayer structures

In-Joon Jeon[a], Dong-Wook Kang[a], Dong-Eon Kim[a,*], Dong-Hyun Kim[b], Sug-Bong Choe[b], Sung-Chul Shin[b]

[a]*Physics Department, Electron Spin Science Center, Pohang University of Science and Technology, Pohang, Kyungbuk 790-784, South Korea*

[b]*Department of Physics, Center for Nanospinics of Spintronic Materials, Korea Advanced Institute of Science and Technology, Taejon 305-701, South Korea*

Abstract

We report the manipulation of magnetic anisotropy in a Co/Pt nano-multilayer (nano-ML) system with particles being embedded. The samples, fabricated by a newly-developed normal incidence pulsed laser deposition (NIPLD) method have salient magnetic characteristics, different from particle-free samples of almost the same structure: (1) they exhibit biaxial magnetic anisotropies and (2) there exists a critical field at which the change in easy direction from a parallel direction to a perpendicular direction and vice versa. By the careful manipulation of particles and nano-layers, we also demonstrate the control of the degree of magnetic anisotropy by embedding particles in a well-defined nano-ML system: uniaxial anisotropy to biaxial one and vice versa. This work, indeed, clearly shows that the integration of nano-building blocks into nano-structures can tailor properties of nano-materials.

Keywords: Magnetic anisotropy; Nano-multilayer structures; Normal incidence pulsed laser deposition

The ever-demanding miniaturization [1,2] has reached a point that the dimensions of sizes in a device are in nanometer scale. However, the working principle in such a scale may not be the same as in a larger scale and is governed by quantum phenomena. The successful application of nano-technology depends upon the detailed understanding of phenomena in a nanometer-scale and the acquirement of control in the fabrication and manipulation of nano-structure building blocks, such as nano-tube [3–5], nano-wire [6–9] and nano-particles [10–18]. Recently, significant progress has been observed in the fabrication and characterization of nano-structures and their manipulations. Magnetic particles [14–18] can affect electron conduction or optical properties of their host, and in turn the host may have an effect on the magnetic properties of the particles. In metals, magnetic particles can produce a large change of the resistance with respect to magnetic field such as a giant magnetic resistance [18]. The fabrication of microelectronics with the capability of recording and storage as well as spin-dependent switching may be made possible by utilizing and embedding magnetic nano-particles in semiconductors.

Here, we report the manipulation of magnetic anisotropy in a Co/Pt nano-multilayer (nano-ML) system with particles being embedded. A Co/Pt nano-ML

* Corresponding author. Tel.: +82-54-279-2089; fax: +82-54-279-3099.
E-mail address: kimd@postech.ac.kr (D.-E. Kim).

0169-4332/02/$ – see front matter
PII: S0169-4332(02)00432-4

system has been studied as a magneto-optical (MO) material. It has been known that a ML system with a Co-layer thickness of ∼0.5 nm and a Pt-layer thickness of ∼1 nm has a uniaxial perpendicular (to its ML surface) magnetic anisotropy; the easy direction of the magnetization is perpendicular to the ML surface. We demonstrate for the first time that the control of layer thickness and the embedment of particles can change the type of a magnetic anisotropy: from a uniaxial type to a biaxial type. We have prepared Co/Pt nano-MLs, with particles being embedded, on a native oxide Si (1 0 0) wafer or a glass substrate under a base pressure of $\sim 1 \times 10^{-6}$ Torr at a room temperature by a newly-developed normal incidence pulsed laser deposition (NIPLD) method [19]. In a conventional PLD, ablating laser beams are incident onto a target at the incidence angle of 45°. During deposition, the direction of a laser plume changes because the craters made by laser ablation modify the surface. Hence, using the conventional PLD, it has been very difficult to produce uniform, well-defined MLs with a thickness of a nanometer or less. The NIPLD has overcome this problem and enables one to fabricate excellent ML-layers with layers of a few tenths of nanometers [19]. The nano-MLs fabricated by NIPLD in this study have 15 bi-layers. The thickness of Co-layer varies from 0.4 to 0.8 nm and that of Pt-layer is ∼1 nm. A small angle X-ray scattering (SAXS) using Cu Kα radiation at 0.154 nm was used to characterize the structures of the samples. The SAXS data of one sample, shown in Fig. 1, reveal sharp Bragg peaks and clear Kiessig fringes, indicating that the layer thickness is uniform and the interface roughness is small. The fitting (the solid line) was done using the dynamical X-ray scattering theory [20,21], yielding that the thickness' of Co- and Pt-layer are 0.57 and 1.3 nm, respectively. The inset in Fig. 1a is the large angle X-ray scattering (LAXS) data, showing that the growth direction of Pt is ⟨1 1 1⟩ and Co-layers do not have any crystalline structure.

The production of particles in PLD has been known [22,23]. The careful control and minimization of laser energy impinging onto a target can lead to the reduction of the number of particles as well as their average size. Laser energy fluence used were 0.38 and 0.42 J/cm^2 for Co and Pt, respectively, for which the deposition rates were about 2.3×10^{-4} and 4.3×10^{-4} nm per shot for Co and Pt, respectively. At this level of deposition process, a majority of particles are in the size of a few to a few tens nanometers in diameter with an estimated density of 1.1×10^9 particles/cm^2 as shown as white dots in Fig. 1b. The density of larger particles is smaller, less than 10^6 particles/cm^2. During the deposition process, these particles are also formed and deposited as atoms are deposited to form

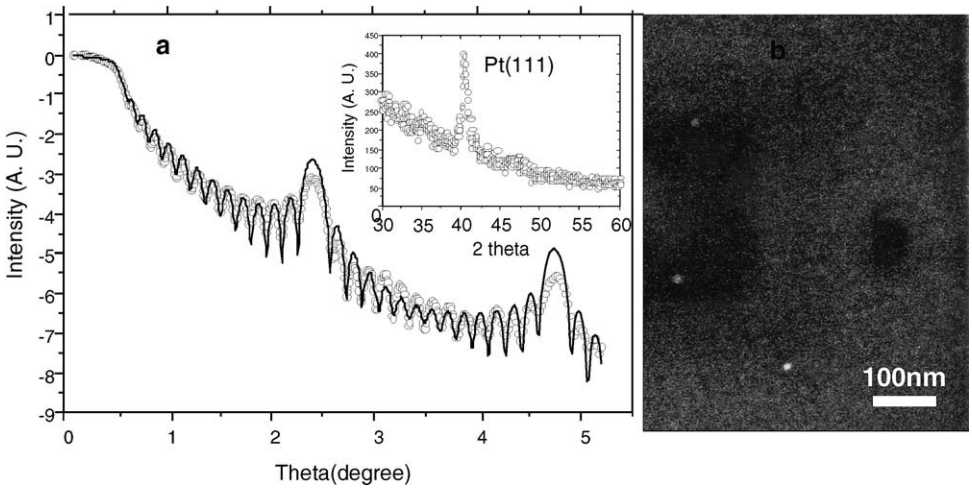

Fig. 1. (a) SAXS data (open circles) showing the well-defined nano-ML structure. The thickness of Co- and Pt-layers are estimated to be 0.57, and 1.3 nm, respectively, by fitting (solid line) using X-ray dynamical scattering theory. An inset is the LAXS data, showing that Pt has a crystalline structure and Co does not. (b) SEM picture: particles (white dots) are shown. The sample was fabricated with a laser fluence of 0.38 and 0.42 J/cm^2 for Co and Pt, respectively. The scale bar is 100 nm.

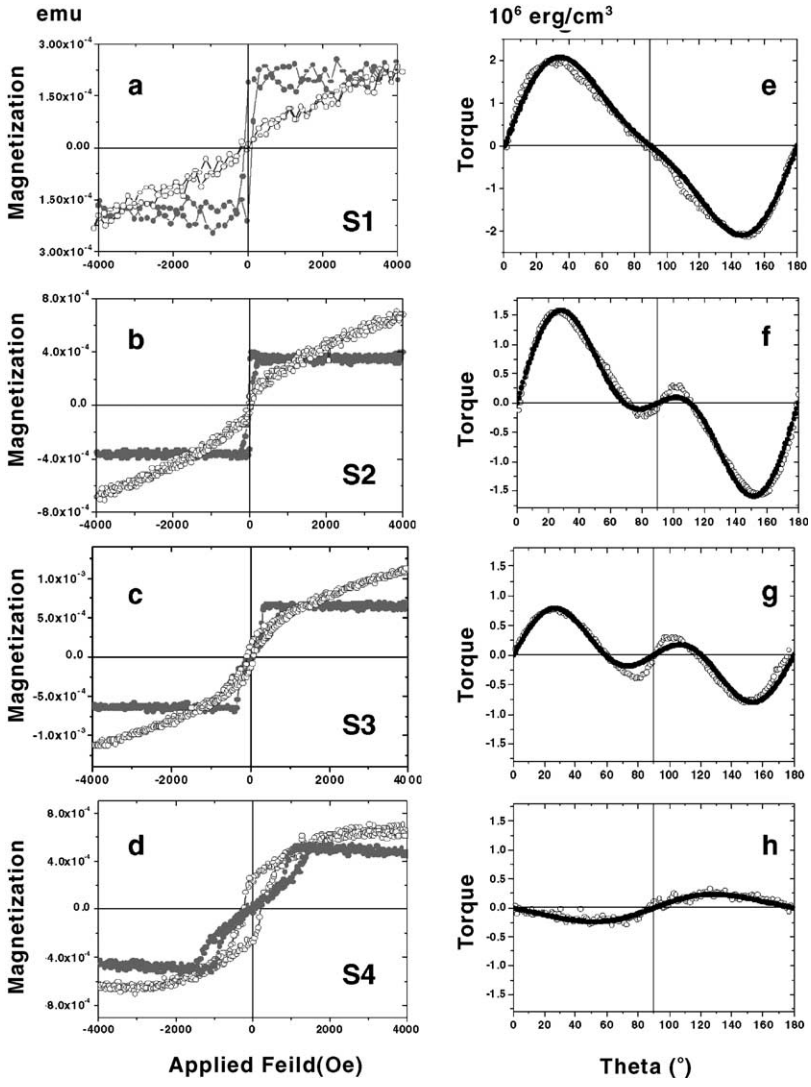

Fig. 2. The magnetizations were measured with a magnetic field parallel (blue circles) and perpendicular (red dots) to the sample surface. The magnetic field of 10 kOe was applied in the torque measurement. S1 was fabricated by a magnetron sputtering system. All other samples were made by PLD. The structural parameters, determined by SAXS are: $d_{Co} = 0.4$ nm, $d_{Pt} = 1.1$ nm for S1 and S2; $d_{Co} = 0.6$ nm, $d_{Pt} = 1.3$ nm for S3; $d_{Co} = 0.7$ nm, $d_{Pt} = 1.0$ nm for S4.

layers. Hence a nano-ML with particles being embedded is fabricated.

The magnetic properties of our samples were characterized by a vibrating sample magnetometer (VSM) and a null-type torque magnetometer (TM). Fig. 2 shows the magnetization behaviors (Fig. 2a–d) measured by VSM and the torque measurements (Fig. 2e–h) at room temperature with an applied field of 10 kOe. Each row represents one sample: its magnetization and corresponding torque measurement. The first sample (S1, Fig. 1a and e) is different from other samples in that it has 10 bi-layers and was fabricated using a magnetron sputtering system where atoms are sputtered and deposited on a substrate. This sample is free of particles. The SAXS measurement of S1 revealed almost the same structure as S2 has. The

magnetization measurements were done with an applied magnetic field perpendicular (solid dots and lines) and parallel (open circles and lines) to the ML surface. As shown in Fig. 2a, S1 shows a paramagnetic behavior in the direction parallel to its surface, on the other hand it reveals the hysterisis in the perpendicular direction, indicating that the easy direction of magnetization is perpendicular to the ML surface. The torque measurement data resembles closely a sine function (Fig. 2e). This is a typical characteristics of the magnetism of Co/Pt MLs with thickness' of Co- and Pt-layers being less than 1 nm, fabricated by either a magnetron sputtering or an e-beam deposition: uniaxial type anisotropy with a perpendicular magnetization. S2 has features similar to and different from S1. A similar feature is that its easy direction of magnetization is perpendicular to its surface, on the other hand different ones that its coercivity is smaller and its magnetic anisotropy is not uniaxial. The torque measurement cannot be fitted by a simple sine function, indicating the additional effect from particles embedded in the nano-ML structure.

Samples with different thickness of Co-layers were also fabricated under the same condition as for S2. As the thickness of a Co-layer increases (or the number of Co particles increases), the ferromagnetic characteristics are developed in the direction parallel to its surface; on the other hand, in the perpendicular direction, the ferromagnetic behavior diminishes (no coercivity field). A salient feature is that there exists a critical magnetic field at which the easy direction of magnetization changes from the parallel direction to the perpendicular direction or vice versa. To our knowledge, this kind of magnetization behavior has never been observed.

The torque measurements of these samples also indicate the change in the property of their magnetic anisotropies since $\Gamma = -\mathrm{d}E_\mathrm{a}(\theta)/\mathrm{d}\theta$, where Γ is the torque and E_a the magnetic anisotropy energy. Assuming that the perpendicular magnetic anisotropy (PMA) due to the interface effect in the ML structure and the in-plane anisotropy due to particles embedded in ML are independent, the magnetic anisotropy energy, E_a can be written by

$$E_\mathrm{a}(\theta) = K_{\mathrm{eff\_ML}} \sin^2\theta + k_{\mathrm{eff\_par}} \sin^2(90-\theta) - M_\mathrm{s}H \tag{1}$$

where $K_{\mathrm{eff\_ML}}$ and $K_{\mathrm{eff\_par}}$ are the effective anisotropy constants due to the ML system and nano-particles, respectively. $K_{\mathrm{eff\_ML}}$ includes the contributions from both bulk and interfaces. θ is the angle between the surface, H the applied magnetic field and M_s the saturation magnetization. The torque is then expressed by

$$\Gamma = -\frac{\mathrm{d}E_\mathrm{a}(\theta)}{\mathrm{d}\theta} = (K_{\mathrm{eff\_ML}} - K_{\mathrm{eff\_par}})\sin(2\theta) \tag{2}$$

The shape of the torque curve is basically that of $\sin(2\theta)$ and the relative strength of the anisotropy constants determines the magnitude and direction of

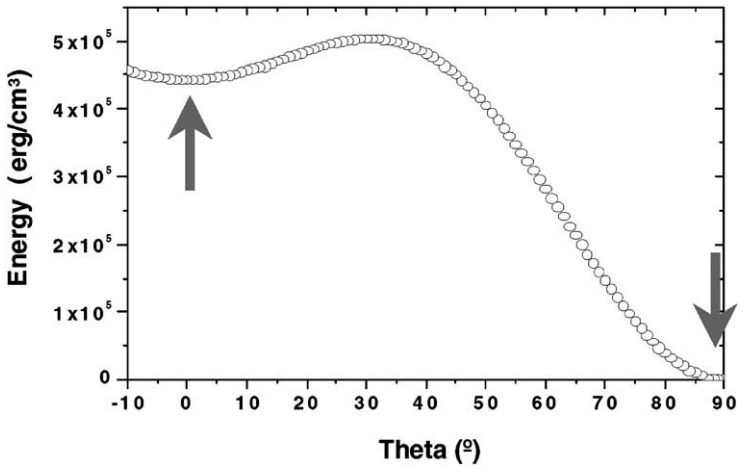

Fig. 3. Magnetic anisotropy energy of S3 with two minima, which correspond to the biaxial anisotropy.

the torque. However, the measured torque curve is substantially different from this model. To represent the additional effect due to particles embedded in the nano-ML structure, the next higher-order term is included in the magnetic anisotropy energy $E_a(\theta)$:

$$E_a(\theta) = K_{eff} \sin^2\theta + K_2 \sin^4\theta - M_s H \quad (3)$$

where $K_{eff} = K_{eff\_ML} - K_{eff\_par}$ and K_2 is the second-order anisotropy constant. Here it is assumed that the direction of a magnetization is nearly the same as that of an applied magnetic field. Using Eq. (3) for the magnetic anisotropy energy, the fittings (solid squares) to the experimental data (open circles) could be done (Fig. 2e–h) to determine the anisotropy constant. The fitting yields that the sign of K_2 as negative, the meaning of which is clear in the plot of $E_a(\theta)$ as shown in Fig. 3 for S3. $E_a(\theta)$ has two minima at $\theta = 0^\circ$ (parallel) and $\theta = 90^\circ$ (perpendicular), which is a good evidence of the existence of two easy directions for magnetization, i.e. biaxial anisotropy.

In conclusion, we have fabricated Co/Pt nano-MLs with particles being embedded and has shown that this sample has different magnetic characteristics from particle-free samples (made by a magnetron sputtering system) of the almost same structure in the following matters: (1) they have smaller coecivity fields, (2) they have biaxial magnetic anisotropies and (3) there exists a critical field at which the easy direction change from a parallel direction to a perpendicular direction and vice versa. We have also demonstrated the capability of engineering a magnetic anisotropy from uniaxial type to biaxial one and vice versa by the combination of particles and nano-layers.

Acknowledgements

This work has been supported in part by the Electron Spin Science Center funded by Korean Scientific and Engineering Foundation and by POSTECH BSRI research fund.

References

[1] P. Peercy, Nature 406 (2000) 1023–1026.
[2] G. Timp, Nanotechnolgoy, Springer, New York, 1999.
[3] C. Dekker, Phys. Today 52 (1999) 22–28.
[4] S.J. Tans, T.M. Verschueren, C. Dekker, Nature 393 (1998) 49–52.
[5] J. Hu, M. Ouyang, P. Yang, C.M. Lieber, Nature 399 (1999) 48–51.
[6] X. Duan, Y. Huang, Y. Cui, J. Wang, C.M. Lieber, Nature 409 (2001) 66–69.
[7] Y. Cui, C.M. Lieber, Science 291 (2001) 851–853.
[8] T. Thur-Albrecht, J. Schotter, G.A. Kastle, N. Emley, T. Shibouchi, L. Krusin-Elbaum, K. Guarini, C.T. Black, M.T. Tuominen, T.P. Russel, Science 290 (2000) 2126–2129.
[9] Y.R. Hacohen, E. Grunbaum, R. Tenne, J. Sloan, J.L. Hutchison, Nature 395 (1998) 336–337.
[10] A.P. Alivisatos, Science 271 (1996) 933–937.
[11] S. Indris, P. Heitjans, H.E. Roman, A. Bunde, Phys. Rev. Lett. 84 (2000) 2889–2892.
[12] T. Bachels, T. Schafer, H.J. Guntherodt, Phys. Rev. Lett. 84 (2000) 4890–4893.
[13] A.A. Shvarstburg, M.F. Jarrold, Phys. Rev. Lett. 85 (2000) 2530–2532.
[14] H. Sato, O. Kitakami, T. Sakurai, Y. Shimada, J. Appl. Phys. 81 (1997) 1858–1862.
[15] R.H. Kodama, A.S. Edelstein, J. Appl. Phys. 85 (1999) 4316–4318.
[16] K.J. Kirk, J.N. Chapman, S. McVitie, P.R. Aitchison, C.D.W. Wilkinson, Appl. Phys. Lett. 75 (1999) 3683–3685.
[17] G.M. Pastor, J. Dorantes-Davila, S. Pick, H. Dreysse, Phys. Rev. Lett. 75 (1995) 326–329.
[18] B.J. Hickey, M.A. Howson, S.O. Musa, N. Wiser, Phys. Rev. B 51 (1995) 667–669.
[19] I.J. Jeon, D. Kim, D.J.S. Song, J.H. Her, D.R. Lee, K.-B. Lee, Appl. Phys. A Rapid Commun. 70 (2000) 235–238.
[20] D.R. Lee, Y.J. Park, D. Kim, Y.H. Jeong, K.-B. Lee, Phys. Rev. B 57 (15) (1998) 8786–8789.
[21] D. Kim, D. Cha, S. Lee, J. Vac. Sci. Technol. A 154 (1997) 2291–2296.
[22] D.B. Chrisey, G.K. Hubler, Pulsed Laser Deposition of Thin Film, Wiley, New York, 1994.
[23] Y. Suda, T. Nishimura, T. Ono, M. Akazawa, Y. Sakai, N. Homma, Thin Solid Films 374 (2000) 287.